Studying the Mechanisms of Titanium Dioxide as Ultraviolet-Blocking Additive for Films and Fabrics by an Improved Scheme

Hongying Yang,[1] Sukang Zhu,[1] Ning Pan[1,2]

[1]*Center of Physics of Fibrous Materials, Dong Hua University, Shanghai 200051, China*
[2]*Division of Textiles and Clothing, Biological and Agricultural Engineering Department, University of California, Davis, California 95616*

Received 5 August 2003; accepted 7 November 2003

ABSTRACT: Titanium dioxide (TiO_2) has good ultraviolet (UV)-blocking power and is very attractive in practical applications because of such advantages as nontoxicity, chemical stability at high temperature, and permanent stability under UV exposure, for example. Development of nanoscience and -technology provides new ways for better treatment for UV-resistant films and fabrics using TiO_2. However, the exact mechanisms of TiO_2 as a UV-blocking additive are still not very clear, and researchers hold different views on this issue. The aim of this investigation was to study systematically the mechanisms of TiO_2 as a UV-blocking additive for films and fabrics. To achieve this goal, the conventional scheme describing light interactions with fabrics was revised based on more recent progress in optical theory, and special experiments and analytic methods were used in the investigation. Several effects attributed to the nanoscale additives were identified. Moreover, detailed analyses based on the results yielded a few important suggestions useful in developing or improving both inorganic UV-blocking agents and the UV-protective films and textiles. © 2004 Wiley Periodicals, Inc. J Appl Polym Sci 92: 3201–3210, 2004

Key words: inorganic UV-blocking agents; additives; films; adsorption; light scattering

INTRODUCTION

More frequent reports of skin cancer have made people increasingly aware of the danger of prolonged exposure to ultraviolet (UV) rays, which account for about 6% of the terrestrial sunlight and, under excessive doses, is proved to cause erythema, certain skin cancers, keratitis, and cataracts. Textiles and sunblocking creams are the common choices to shield against UV radiation, although UV radiation also weathers and degrades the textiles. Consequently, new UV-blocking agents have been developed to add to or to improve the UV-protective function of textiles, plastic films, and other related products.[1]

There are both organic and inorganic UV blockers. The organic blockers are also called UV absorbers because they mainly absorb UV rays. Inorganic UV blockers are usually certain semiconductor oxides such as TiO_2, ZnO, SiO_2, and Al_2O_3, for example. Compared with the existing organic UV absorbers, the inorganic UV agents are more preferred because of their unique features including, among others, nontoxicity and chemical stability under both high temperature and UV-ray exposure.

However, the mechanism of UV-blocking function of inorganic materials is so far not very clear and researchers hold different views concerning its nature. Take TiO_2, for example: some investigators believe that it provides good UV protection by reflecting and/or scattering most of the UV-rays through its high refractive index.[2,3] Others believe that it absorbs UV radiation because of its semiconductive properties.[4–6] Still others claim that, of a pile of TiO_2 powder, only the nanosize particles absorb UV radiation, whereas the submicrometer-size particles do very little.[7] Given the mixed and often conflicting views, it appears desirable for a thorough investigation on the problem.

This article reports the systematic investigation of the exact mechanisms of TiO_2 as an inorganic UV-blocking additive for fabrics. To obtain more accurate results, an improved scheme on light–object interactions based on recent progress in optical theory was proposed, describing how fabrics or films react to the light illuminating on them. As shown below, this approach yields more informative data than do the conventional approaches and also has the potential to provide deeper understanding and thus improve the optical properties of textiles. Naturally, the new methods described in this article are applicable for studying

Correspondence to: S. Zhu (zusukang@dhu.edu.cn).

Journal of Applied Polymer Science, Vol. 92, 3201–3210 (2004)

the mechanisms of other inorganic UV-blocking additives for fabrics.

EVALUATION OF UV-PROTECTIVE PROPERTY OF FABRICS

A UV-ray, like visual light (VIS), is a segment of the electromagnetic spectrum, with a wavelength ranging from 100 to 400 nm, and is conventionally subdivided into three bands: UVA (320 or 315 to 400 nm), UVB (290 to 315 or 320 nm), and UVC (100–290 nm). The terrestrial solar UV received consists of only UV with wavelength 290–400 nm because UVC and some UVB are absorbed by the stratospheric ozone in the earth's atmosphere.

In recent years, investigators and manufacturers have paid increasing attention to understanding the solar UV-protective properties of textiles. Several related standards have been published by Australia/New Zealand, Europe, and the United States, respectively.[8–10] Among these standards, UPF, T_UVA, and T_UVB are the commonly adopted indices.

The so-called UV-protection factor (UPF) is defined as

$$\mathrm{UPF} = \frac{\int_{290}^{400} E_\lambda S_\lambda \, d\lambda}{\int_{290}^{400} E_\lambda S_\lambda \cdot \tau_\lambda d\lambda} \tag{1}$$

where λ represents the wavelength in nm, E_λ is the relative erythemal effectiveness, S_λ is the solar UV spectral irradiance in W m^{-2} nm^{-1} (data from Albuquerque, NM are used in this study), τ_λ is the spectral transmittance of the specimen, and $d\lambda$ is the wavelength increment in nm.

When $d\lambda$ is constant, three more indices can be calculated by

$$\mathrm{T\_UVA} = \frac{1}{m}\sum_{315}^{400} \tau_\lambda \quad \mathrm{T\_UVB} = \frac{1}{n}\sum_{290}^{315} \tau_\lambda \quad \mathrm{T\_VIS} = \frac{1}{k}\sum_{400}^{760} \tau_\lambda \tag{2}$$

where T_UVA, T_UVB, and T_VIS (in %) are the means of transmittance under UVA, UVB, and VIS (400–760 nm); and m, n, and k stand for the number of measurement points for UVA, UVB, and VIS, respectively.

In fact, the UPF value represents how much longer people can become exposed wearing clothing, versus not wearing it, until the skin develops reddening.

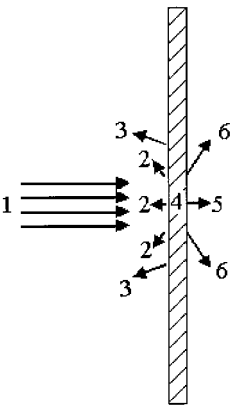

Figure 1 Model of fabric–light interactions.

AN IMPROVED SCHEME ON FABRIC AND LIGHT INTERACTIONS

Conventionally, a light illuminating on fabric was divided into three parts according to the resulting light distribution: reflection, absorption, and transmission. A more detailed division was made by subdividing the transmission part into a component that passes through the pores and a diffused or scattered component.[1] This description is useful in evaluating the optical properties of fabrics, but is not so useful in analyzing the origin of fabric optical properties. This article thus advocates an improved scheme based on optical theory, and this study focuses on both plastic films and textile fabrics.

In examining the interactions between light and fabrics, the incident light normally illuminating a fabric is divided as follows (see Fig. 1): part of the light turns into regular reflection (including specular and diffused reflection) at the interface, marked as *dr*; another part *a* enters into the fabric and is absorbed by the material; some passes through the fabric with direction unchanged, recorded as *dt*; whereas another part enters into the fabric and is scattered because of the uneven structure of the fabric and/or the additives in the fabric. Of the scattered light, the backward-scattered light generates the same effect as the reflection, termed scattered reflection *sr*, whereas the forward-scattered light also passes through the fabric; portions maintaining the same direction as that of the incident ray are recorded as *dt*; the rest, deviating from the incident direction, are termed as diffused (or scattered) transmission *st*.

It can be seen that the improved scheme adds the factor of scattered light to the analysis, which is then subdivided into scattered reflection, direct transmission, and diffused transmission according to their final effects. In short, the normal incident light is eventually transferred into five portions, as follows: regular reflection, scattered reflection, absorption, direct transmission, and diffused transmission. As a matter of

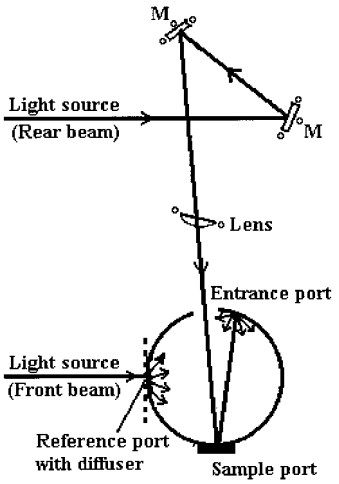

Figure 2 Light path of integrating sphere in Cary 500 spectrophotometer.

fact, scattering is an indispensable part of the interactions between a medium and light, and it plays an important role in determining the optical behavior of fabrics.

According to the new scheme, the following relations hold:

$$R = dr + sr \quad A = a \quad T = dt + st \quad I = R + A + T \tag{3}$$

where R is the total reflection, A is the absorption, T is the total transmission, and I is the incident ray, so that

$$\rho = R/I \quad \tau = T/I \quad s\tau = st/I \quad \alpha = A/I = 1 - \rho - \tau \tag{4}$$

where ρ is the reflectance, τ is the transmittance, $s\tau$ is the scattered transmittance, and α is the absorbance. Among these variables, ρ, τ, and $s\tau$ can be measured using a spectrophotometer with an integrating sphere, and α can then be calculated by eq. (4). Figure 2 shows the path of a Φ 110-mm integrating sphere in a Cary 500 spectrophotometer from Varian Technologies (Palo Alto, CA).[11]

The new scheme as well as the characteristic features ρ, τ, $s\tau$, and α are fundamental in identifying and analyzing the contributions of various interactions between light and fabric containing TiO_2, so as to explore the true mechanisms of TiO_2 as a UV-shielding additive. Further, they are of great advantage, as shown later, in studying fabric optical behaviors to explore new methods in improving or adjusting the optical properties of fabrics.

EXPERIMENTAL

Materials and tests

Four commercial TiO_2 powders, B, D, H, and P were used in this study. To obtain reliable data, several important characteristics of the powders themselves were tested.

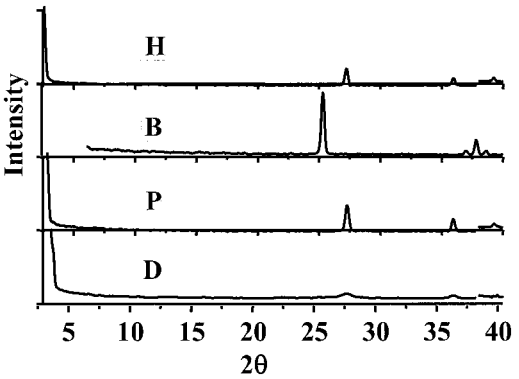

Figure 3 XRD patterns of TiO_2 of different types: H, B, P, and D.

First, the crystallinities of the powders were determined through X-ray diffraction (XRD) using a DMAX/rB diffractometer (Rigaku Co., Tokyo, Japan). The XRD patterns are given in Figure 3 showing that D, P, and H are rutile TiO_2, whereas B is an anatase TiO_2.[12] Meanwhile, the diffraction peak of D is clearly broader than that of the others, and its mean diameter, calculated by using Scherre's eq. (7), was about 32 nm. Second, using a nitrogen absorbance meter, model JB-1 (made in China), the Brunauer–Emmett–Teller (BET) specific surface areas of the powders were measured, ranging from 139, 11, 6.4, and to less than 1 m^2 g^{-1} for D, P, B, and H, respectively. Under the assumption that the particles are spherical, their average diameters were thus calculated. D is about 32 nm in diameter, consistent with the result calculated by Scherre's equation with the line broadening. B and P are in the submicrometer range, although B is slightly smaller than P; and H is at the micrometer scale. Meanwhile, the primary diameter of D was also mea-

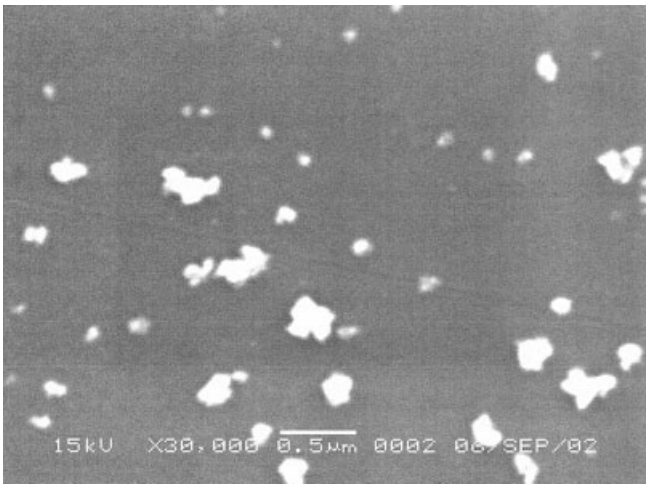

Figure 4 SEM micrograph of sample D.

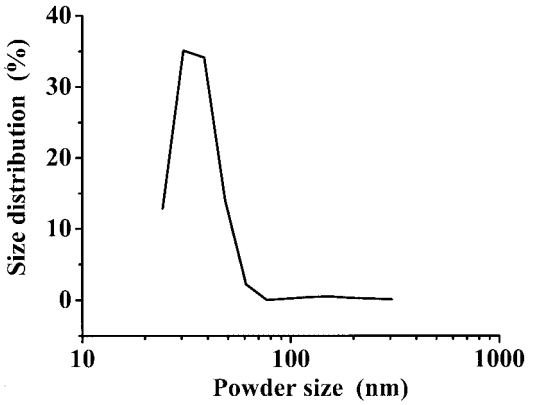

Figure 5 Size distribution of sample D in water.

sured by a scanning electron micrograph and is actually <100 nm (see Fig. 4). Furthermore, the size distribution by number for powder D in deionized water was analyzed by a Zetasizer3000HS (Malvern Instruments, Worcestershire, UK) using the laser-diffraction method, shown in Figure 5. A test summary for the four powders is listed in Table I.

Additional materials were also used in this investigation, including a polymer binder from National Starch and Chemical (Berkeley, CA), marked as j below; an ordinary commercial organic UV absorber used as a reference, denoted as O, as well as some cotton fabrics are listed in Table II.

Preparation of the TiO_2 composite films

TiO_2 powders were dispersed in deionized water and stirred with ultrasonic agitation (20 kHZ) for 5 min. Then, the binder j was mixed uniformly into a sol or suspension for 5 min by ultrasonic stirring as well. Certain amounts of these mixtures were applied onto a level glass sheet, and solidified into films at room temperature. The films were then peeled off carefully from the glass and placed into sample holders and cured under standard conditions for 24 h before testing. Table III provides details concerning all the films, and special care was taken during the preparation to ensure their consistency. The weight percentages in Table III represent the ratio of powder to the pure binder. The thickness of the films was about 0.1 mm, similar to the thickness of light fabrics.

Treatment of the tested fabrics

Three types of cotton fabrics, denoted as t, p, and g, respectively, in Table II, were used in the study. Fabrics t and p were finished white cotton fabrics without special whitening treatment to avoid the influence of the whitening agents; fabric g was of originally gray cotton and served as the untreated reference sample, which was dipped in water and then padded and dried so as to minimize the effect of water shrinkage. Fabrics t, p, and g were each given a simple UV-protective finishing in the lab: dipped in 2 wt% D or P aqueous suspension (dispersed uniformly by the ultrasonic method), then padded with about 100% pick-up and dried. Table II gives the specifications of the fabrics. The untreated and treated fabrics were balanced under standard conditions for 24 h before measurement.

Equipment and measurement[13–16]

A Cary 500 spectrophotometer, with a Varian integrating sphere (Palo Alto, CA) mentioned earlier, was chosen to measure the UV–VIS interactions of the materials listed in Tables II and III. The following spectra were scanned between 200 and 800 nm with a 1-nm interval at room temperature, including the reflection spectra of the powders, and the reflection spectra, transmission spectra, and scattered transmission spectra of both films and fabrics.

RESULTS AND DISCUSSION

UV properties of TiO_2 powders

Figure 6 gives the reflectance spectra of the four TiO_2 powders. The absorption capacity and absorption ranges of powders can be obtained from their reflectance spectra. Clearly, all four TiO_2 powders—the nano-TiO_2 D, the submicron-TiO_2 B and P, and micron-TiO_2 H—absorb UV rays, which is in conflict with the conclusion from Zhang and Mou[7] that submicron-TiO_2 absorbs virtually no UV rays.

In fact, the UV-absorption property is a natural attribute of TiO_2, which can be explained by the solid band theory. TiO_2 is a kind of semiconductor oxide with a large band gap between its low-energy valence band and its high-energy conduction band. The band

TABLE I
Descriptions of the Four TiO_2 Powders

Feature	D	B	P	H
Appearance	White, puffed	White powder	White, with a little agglomeration	White, with some agglomeration
Crystal phase	Rutile	Anatase	Rutile	Rutile
Size grade	Nanosized	Submicron	Submicron	Micron

TABLE II
Specifications and Symbols of the Fabrics

Fabric specification	Thickness (mm)	Untreated	Treated with D	Treated with P
21 × 21, 108 × 58 white cotton twill	0.50	t	Dt	Pt
40 × 40, 64 × 72 white cotton plain	0.30	p	Dp	Pp
21 × 21, 83 × 48 gray cotton twill	0.55	g (dipped and padded with water, then dried)	Dg	Pg

gaps for rutile and anatase are 3.0 and 3.2 eV, respectively, corresponding to the absorption edges 413 and 388 nm.[17] When TiO_2 is illuminated by light with energy higher than its band gaps (i.e., with wavelength shorter than the absorption edges), the electrons will absorb the energy of the photons and be excited to cross the band gap, so as to produce the pairs of electrons and holes. These excited electrons and holes will then result in two competing consequences: either combing with other holes or electrons, or being captured by the absorbents surrounding TiO_2 and initiating reduction and oxidation reactions. The former explains how the UV-protector TiO_2 functions, whereas the latter reveals the mechanism of TiO_2 as a light catalyzer.

Next, the differences in internal structure between rutile and anatase are reflected in their properties. For instance, the density of rutile (4.25 g/cm^3) is higher than that of anatase (3.89 g/cm^3), and the band gap of rutile is also narrower than that of anatase. As a result, rutile has much higher excited electron–hole recombination probability and substantially lower light-catalyzing activity than that of anatase. Thus, rutile is more suitable for being used as a UV blocker, whereas anatase is more suitable for being a light catalyzer.

In addition, the UV-blocking or light-catalyzing function can and should be altered through different surface modifications corresponding to different applications. For instance, without further modification it is known that anatase TiO_2 as a delusterant for synthetic fiber in fact accelerates the light degrading and weathering of the synthetic fiber.[18]

The absorption peaks of D, P, B, and H are estimated from Figure 6, by using the method proposed by Fochs,[19] as 398, 384, 411, and 411 nm, respectively. The nano-TiO_2 D (rutile) exhibits more than 10-nm blue shift compared with that of the ordinary TiO_2. Meanwhile, among powders D, P, B, and H, the nano-particle D shows the strongest absorption power, B the second strongest, followed by pigments P and H.

The strengthened absorption and blue shift of the absorption peak of nano-TiO_2 result from certain unique effects of nanomaterials, such as the quantum-size effect, nanoscale effect, and quantum field emission effect.[7] Strengthened UV absorption is beneficial to UV blocking, whereas the blue shift of the absorption peak reduces absorption of UV-rays of longer wavelength and is thus undesirable for solar UV protection. Although the erythemal hazard of long-wavelength UV is lower than that of short-wavelength UV, the former penetrates deeper into the skin and has an accumulating effect on the skin. Thus, when TiO_2 is used as a solar UV blocker, certain techniques should be adopted to generate a red shift to eliminate or offset the blue shift for better UV protection.

Functions of TiO_2 in films

TiO_2/binder composite films were used in this study, thus conferring several benefits. First, the films can be viewed as simplified substitutes for fabrics, removing the effect of porous and fuzzy fabric structures. Second, the internal structures of TiO_2/binder composite films are formed through simple physical mixtures, as evidenced from the derivative spectra of reflectance of D, j, and Dj shown in Figure 7; the edges of Dj corresponds to that of j or D, and no new peak formed; thus, the changes in optical properties of the composite film compared with that of pure binder film should be attributed solely to the additive TiO_2. Third, TiO_2/binder composite films can also reflect the effect of TiO_2 filling inside the matrix. Fourth, because the refractive index of the binder j (1.5 or so) is close to that of most fibrous materials (1.5–1.6), this avoids the otherwise complicity on light-scattering analysis. Finally, because the absorption peaks of binder j are

TABLE III
Films Prepared and Their Symbols

Symbol	j	Dj	Bj	Pj	Hj	Oj
Film composition	Binder	j + 2%D	j + 2%B	j + 2%P	j + 2%H	j + 2%O
Symbol	Dj1	Dj2	Dj3	Pj1	Pj2	Pj3
Film composition	j + 1%D	j + 2%D	j + 3%D	j + 1%P	j + 2%P	j + 3%P

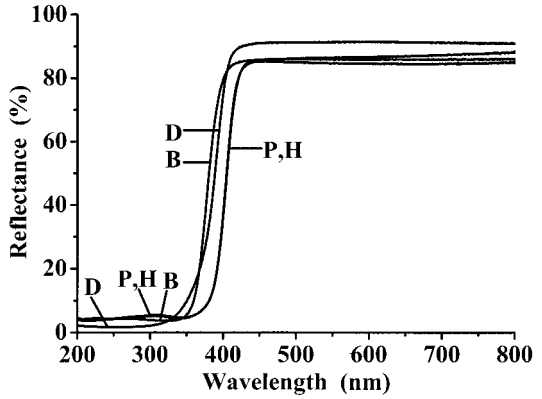

Figure 6 Reflectance spectra of four TiO_2 powders.

both shorter than 290 nm, it presents almost negligible interference in studying the optical properties of TiO_2 in the region of 290–760 nm.[20,21]

Figure 8 shows the transmission (including the diffused transmission), the absorption, and reflectance spectra of the films. Within the band of UV, the four TiO_2 composite films show a significant decrease in transmittance, compared with that of the pure binder film j (i.e., TiO_2 exerts a considerable influence in improving the film's UV-blocking property). The reason becomes clear by analyzing both Figures 8 and 9. First, TiO_2 composite films have strong absorption in the band of 290–350 nm, with Dj having the strongest absorption among them. Next, in the band of 350–400 nm, besides absorption, composite films' strong scattering power also plays a role in reducing transmittance. The forwardly strong scattering can be demonstrated by the high ratio, $s\tau/\tau > 90\%$, for all TiO_2 composite films, whereas $s\tau/\tau$ values of the reference films j and Oj are only 7 and 8%, respectively, estimated from Figure 8. Note that the ratio $s\tau/\tau$ reflects the light transmission caused by scattering relative to the total. The backward scattering, on the other hand, increases light reflectance, which helps in blocking

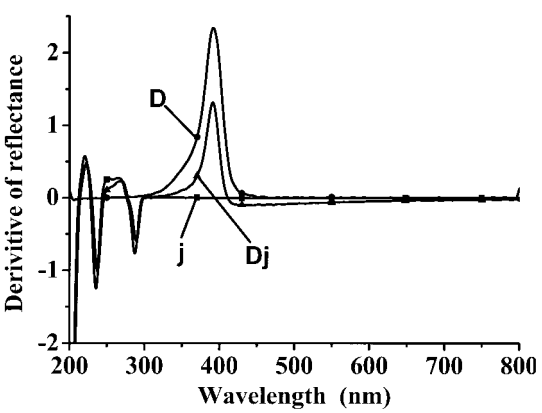

Figure 7 Derivative of reflectance of j, D, and Dj.

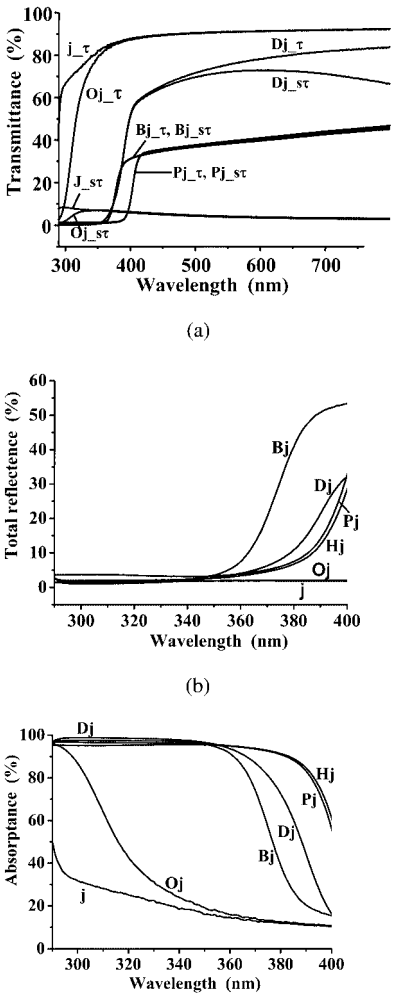

Figure 8 Spectra of films: (a) transmission and diffuse transmission spectra; (b) reflection spectra; (c) absorption spectra.

UV. Compared with pure film j, TiO_2 composite films have enhanced capacity in reflectance ρ from 6 to 28%, shown in Figure 9, whereas the organic UV composite film Oj shows little increase. In other words, TiO_2 composites gain their excellent UV-blocking power mainly from TiO_2's UV-absorption capacity, in addition to some scattering/reflection effects in the long-wavelength band of weak UV absorption or even non-UV absorption for TiO_2.

As in the band of VIS, although all TiO_2 composite films show strong light scattering with $s\tau/\tau$ values $> 90\%$, estimated from Figure 8, the $s\tau/\tau$ for Dj is slightly smaller, indicating that nanopowders have weaker scattering power to VIS than the submicrometer-size and micrometer-size powders. Furthermore, Dj has the highest T_VIS among the four TiO_2 composite films, nearly transparent, whereas the T_VIS values of the other films are all <50%. In fact, the specimen P of only 1% additive reduces by half of the

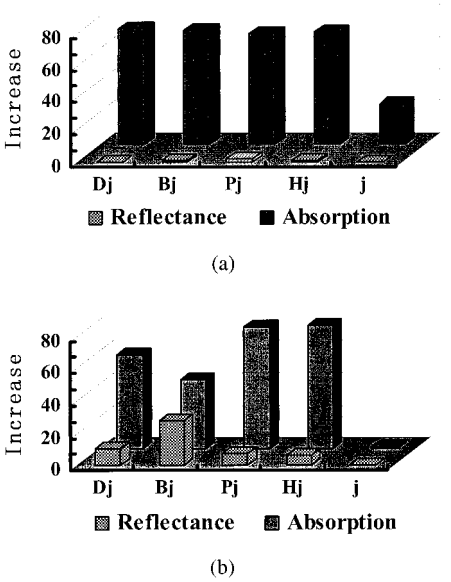

Figure 9 Increase in average reflectance and average absorptance of the composite films compared with the pure binder film: (a) in the band of 290–350 nm; (b) in the band of 350–400 nm.

T_VIS value compared with that of the pure binder film [see Fig. 10(a) and (b)[22]]. These all agree with the light scattering theory and indicate that nanoparticles affect the film color far less than the ordinary scale particles. In addition, the UPF value of Dj1 is >50 and that of Pj2 is >30, which confirms the strong UV absorption power of nano-TiO_2.

According to theory, as light is transmitting in a nonhomogeneous medium, where the refractive index varies at different locations, light scattering will occur. When particles are dispersed in a film matrix, the scattering intensity depends on such factors as the content, the size (diameter d), and the relative refractive index of the particles to the matrix; the higher the relative refractive index, the more actively the light scatters.

When $d < 0.1\lambda$, the Rayleigh scattering theory becomes applicable; the scattering intensity is directly proportional to d^6, and is inversely proportional to the number of particles. The intensity of backward scattering tends to be equal to that of the forward scattering. With the increase of d, the Mie theory is more relevant, given that the forward scattering becomes stronger and the backward scattering turns weaker. The total scattering intensity increases to the peak value when d reaches about $\lambda/2$, and then decreases with further increases of d.

Rutile TiO_2 has a very high refractive index of 2.76 at 589.3 nm wavelength, and 3.03 at 435.8 nm light.[23] The index peaks near the absorption boundary, then decreases sharply and remains low over the absorption band. Therefore, composite films with TiO_2 added have high relative refractive index and cause strong light scattering in the nonabsorption bands such as VIS or near.

It is also easily understood that the scatter intensity to VIS of nanoparticles is far weaker than that of submicrometer-size particles (i.e., a smaller diameter d leading to weaker scatter intensity, less influence on film color, and higher scatter power in blocking light). However, when the diameter decreases to a certain degree, backward-scattering intensity starts to level off, whereas the light-catalytic activity will increase. Thus for TiO_2 UV protector, a particle scale that is too small will in fact abate its performance.

Functions of TiO_2 in fabrics

Figures 11, 12, and 13 present the transmission spectra, UPF values, absorption, and $R/(R + T)$ for fabrics t, p, and g, respectively.

It is easily seen in these figures that the untreated fabrics themselves can reflect, scatter, and absorb some UV, but not enough for desired protection. For instance, the UPF value for thick fabric t is 9 in Figure 11(b), only 3 for thin fabric p in Figure 12(b), and is 19 in Figure 13(b) for the gray fabric g, attributed to the sizing stuffs binding on the warp yarns and the natural pigments, lignins, on the cotton fibers absorbing some UV.

After treatment with TiO_2, either the nanosize (D) or the submicron-size (P), the UV-blocking properties of the fabrics improve greatly in all three indices. The

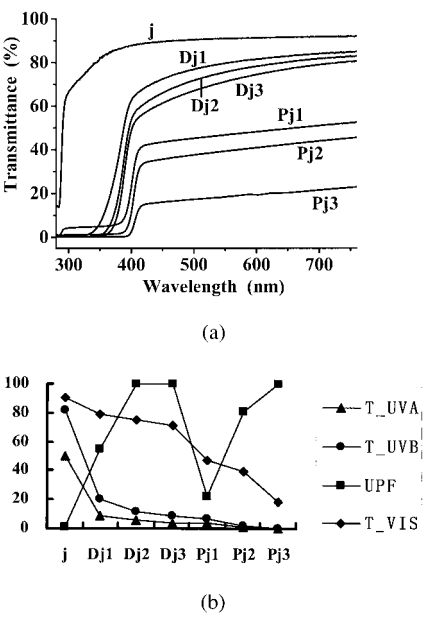

Figure 10 Comparison between composite films with different contents of TiO_2[22]: (a) transmittance spectra for various samples; (b) other optical parameters for various samples. (UPF value is recorded as 100 once over 100.)

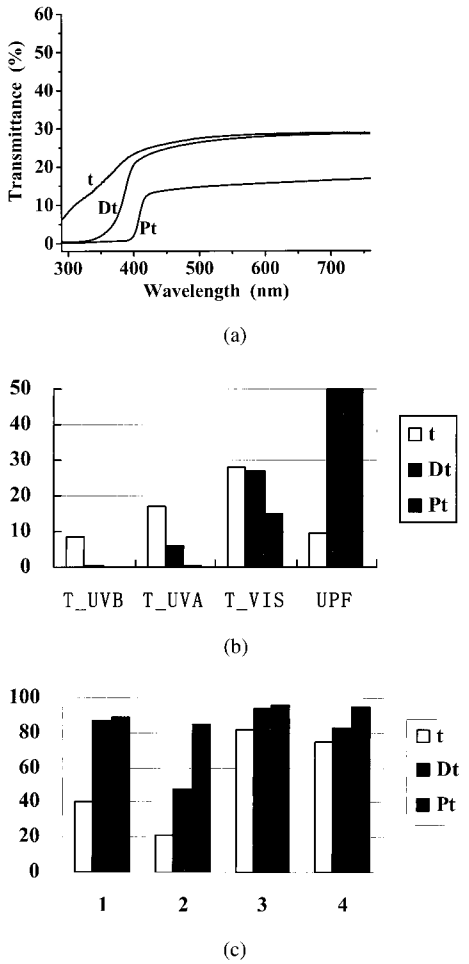

Figure 11 Comparison between untreated and treated white twill cotton (t): (a) transmittance spectra for untreated and treated samples; (b) important optical indices for untreated and treated samples; (c) other optical parameters for untreated and treated samples.

UPF values for the three types of the fabrics all exceed 50, and even the lowest UPF increases from 3 to 26 for the untreated fabric p. In the band of 290–350 nm, the absorption power of nano-TiO_2 is stronger than that of the pigment-TiO_2. The case is opposite in the band of 350–400 nm because of the blue shift at the absorption edge of nano-TiO_2. Direct transmittance ($\tau - s\tau$) values for treated fabrics are all smaller than those of their corresponding untreated fabrics. $R/(R + T)$ values of treated fabrics increase compared with those of the untreated fabrics, indicating a strengthening of the scattering/reflection effect [see the corresponding (c) parts of the figures for each fabric].

Meanwhile, the increase in scattering in treated fabrics with TiO_2 is not as remarkable as that in TiO_2 composite films because the uneven and porous fabric structures already provide some inherent scattering capacity. According to our calculation, $s\tau/\tau$ values for untreated fabrics are above 90%, whereas the $s\tau/\tau$ ratio for the pure film j is even below 10%. Therefore, similar to the conclusion discussed earlier (see experimental section), the improvement of UV-blocking function for the treated fabrics results to a great degree from the UV absorption of TiO_2, and the scattering and reflection exert only a marginal effect, less than that in the films.

In addition, the gray fabric g treated with D has a higher UPF value than that treated with P. On the one hand, it is attributed to the stronger UV absorption of D; on the other hand, it reflects the better affinity of D toward fabrics and particularly toward the sizing stuffs (binders). This is beneficial for normal UV-protective finishing, which needs some binders to bond TiO_2 better to fabrics. In fact, during the process of UV-protective finishing, we have found that D had much better affinity to fabrics than P, and P in fact easily fell off the fabrics. This confirms that nanoparticles possess better affinity to fabrics than those of larger scale because of their huge surface area to volume ratio and high surface energy.

When comparing the optical property in the VIS band in the corresponding (b) parts of the figures

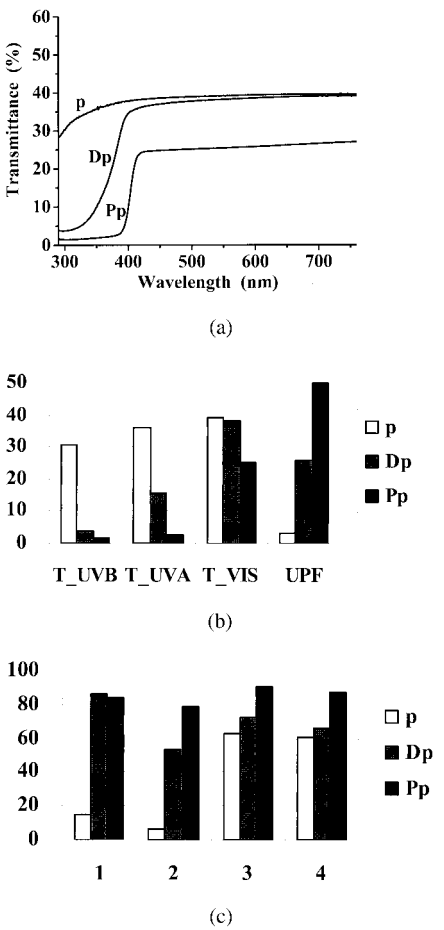

Figure 12 Comparison between untreated and treated white cotton plain (p): (a) transmittance spectra for untreated and treated samples; (b) important optical indices for untreated and treated samples; (c) other optical parameters for untreated and treated samples.

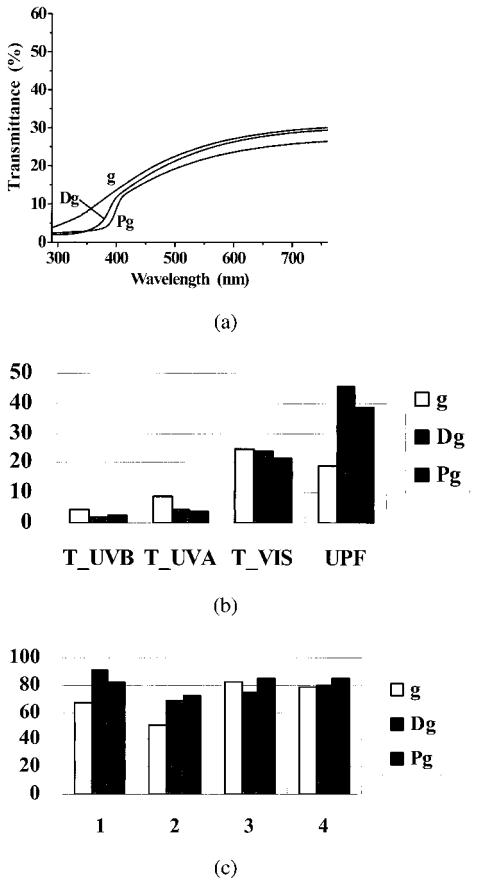

Figure 13 Comparison between untreated and treated gray cotton twill (g): (a) transmittance spectra for untreated and treated samples; (b) important optical indices for untreated and treated samples; (c) other optical parameters for untreated and treated samples (1, average absorptance in the band of 290–350 nm; 2, average absorptance in the band of 350–400 nm; 3, average $R/(R + T)$ in the band of 290–350 nm; 4, average $R/(R + T)$ in the band of 350–400 nm). UPF value is recorded as 50 once over 50.[24]

(taking T_VIS value for example), fabrics treated with D show little difference from their corresponding untreated fabrics, whereas fabrics treated with P reduce their T_VIS values to about one third of those of the corresponding untreated fabrics. Actually, fabrics treated with D show little change in appearance, whereas fabrics treated with P present a visible whitening effect, attributed to the white pigment.

CONCLUSIONS

1. As the experimental results show, regardless of the particle sizes, TiO_2 clearly absorbs UV radiation, which can be explained by the solid band theory. This is different from the previous view that submicron-TiO_2 absorbs little UV. Also, TiO_2 works as a UV-blocking additive mainly through UV absorption, and the scattering and reflection mechanisms are significant only in the band where TiO_2 has either weak or nonabsorption, although TiO_2 has a higher refractive index than that of most other semiconductors. Therefore, it can be expected that other inorganic semiconductor oxides with UVA and UVB absorption capability, like ZnO, should have a similar function mechanism to that of TiO_2 when used as UV-ray blockers for fabrics.
2. Because of its stronger UV absorptance, nanoscale TiO_2 exhibits better UV-blocking capacity than that of the pigment TiO_2; moreover, it also exerts very little influence, when embedded, on matrix color because of its much weaker scattering intensity to VIS than that of pigment TiO_2. The nanoscale TiO_2 also presents good affinity to fabrics because of its very large specific surface area and high surface energy and activity. However, the blue shift of the absorption edge of nano-TiO_2 is disadvantageous when used as a solar UV protector because it reduces the absorption of UVA near VIS. Nevertheless, these nanoscale effects provide new ways for inorganic UV-blocking agents like TiO_2 to work more effectively in textiles. Of course, other effects of nano-TiO_2 on textiles, such as fabric hand, breath capacity, and so forth, should be given further study.
3. From this study, some useful knowledge has been attained in developing inorganic UV blockers for UV-protective textiles. First, for UV protector nano-TiO_2 it is desirable to strengthen the red shift and offset the blue shift phenomena for more effective solar UV protection. Second, all inorganic UV-blocking agents with the same UV-protective mechanism as that of TiO_2 can work well both exteriorly and interiorly for ordinary UV-protective fabrics, but will not work for camouflage fabrics that require high UV reflectance. Third, when deciding the optimal size of TiO_2 as a UV protector, we should consider both its UV-absorption property and its scattering characteristics. It is biased to selecting the optimal diameter only by light-scattering equations, as done in Wu et al.[24] Fourth, although the scatter effects of TiO_2 exhibit only a marginal effect on fabrics' UV-blocking function, this differentiates TiO_2 from organic UV absorbers. The existing models for predicting the UV-protective effects of fabrics treated with organic UV absorbers are thus not applicable for fabrics with TiO_2.
4. Based on the interactions of fabric to light, the improved model in this study, elucidating in great detail how fabric reacts to light, is more informative and useful in analyzing the UV-blocking mechanisms of TiO_2. The new model

and the analyzing method are also applicable for investigating the mechanism of other inorganic UV-blocking additives for fabrics. Furthermore, the new model is more robust for studying the optical properties of fabrics, analyzing the factors involved, and exploring new methods for further improvement.

References

1. Reinert, G.; Fuso, F.; Hilfiker, R.; Schmidt, E. Text Chem Color J 1997, 29, 38.
2. Mossotti, R.; Innocenti, R.; Dimechelis, R.; Pozzo, P. D. In: Changes in the Properties of Wool Fibres by Using Alternative Materials, Proceedings of the 10th International Wool Textile Research Conference, Aachen, Germany, Nov. 26–Dec. 1, 2000; Vol. 11, F1–P15, 1–9.
3. Bohringer, B. In: UV Protection by Textiles, Proceedings of the 37th International Man-Made Fibres Congress, Dornbirn, Austria, 1998; Vol. 9, pp. 1031–1044.
4. Gupta, K. K.; Tripathi, V. S.; Ram, H.; Ray, H. Colourage 2002, 6, 35.
5. Thiry, M. C. AATCC Rev 2002, 6, 13.
6. Wedler, M.; Hirthe, B. Chem Fibers Int 1999, 49, 528.
7. Zhang, L.; Mou, J. Nano-materials and Nano-structure; Science Press: Beijing, 2001; p. 84.
8. AS/NZS4399:1996. Sun Protective Clothing—Evaluation and Classification (Australia/New Zealand), 1996.
9. AATCC183:1998. Transmittance of Blocking of Erythemal Weighted Ultraviolet Radiation Through Fabrics (Europe), 1998.
10. EN 13758:2001(E). Textiles—Solar UV Protective Properties (United States), 2001.
11. Bortoli, S.; Brill, R.; Edwards, D. Cary Diffuse Reflectance Accessory Service Manual 16, Palo Alto, CA.
12. Joint Committee on Powder Diffraction–International Centre for Diffraction Data (JCPDS-ICDD). Powder diffraction file (PDF). Swarthmore, PA, 1980; pp. 21-1273, 21-1276.
13. Gambichler, T.; Bader, A.; Avermaete, A.; Altmeyer, P.; Hoffmann, K. J Eur Acad Dermatol Venereol 2001, 15, 371.
14. Gambichler, T.; Bader, A.; Avermaete, A.; Bader, A.; Herde, M.; Altmeyer, P.; Hoffmann, K. Photodermatol Photoimmunol Photomed 2002, 18, 135.
15. Gies, P.; Roy, C.; McLennan, A.; Pailthorpe, M.; Hilfiker, R.; Osterwalder, U.; Monard, B.; Moseley, H.; Sliney, D.; Wengraitis, S.; Wong, J.; Human, S.; Bilimis, Z.; Holmes, G. Photochem Photobiol 2003, 77, 58.
16. Hoffmann, K.; Kesners, P.; Bader, A.; Avermaete, A.; Altmeyer, P.; Gambichler, T. Skin Res Technol 2001, 7, 223.
17. Mo, S. D.; Ching, W. Y. Phys Rev B 1995, 51, 13023.
18. Bever, P. M.; Breiner, U.; Conzelmann, G.; von Bernstorff, B.-S. Chem Fibers Int 2000, 50, 176.
19. Fochs P. D. Proc Phys Soc 1956, B69, 70.
20. Cowie, J. M. G.; Rodden, G. I. Polymer 2002, 43, 3415.
21. Ikake, H.; Hashimoto, W.; Kawai, M.; Kamiyama, N.; Shimizu, S.; Kurita, K.; Yano, S. Kobunshi Ronbunshu 2002, 59, 539 (in Japanese).
22. Laperre, J.; Gambichler, T.; Driscoll, C.; Bohringer, B.; Varieras, S.; Osterwalder, U.; Rieker, J.; Camenzind, M.; Hoffmann, K. Photodermatol Photoimmunol Photomed 2001, 17, 223.
23. DeVore, J. R. J Opt Soc Am 1951, 41, 416.
24. Wu, D.; Du, Z.-L.; Gao, X. Nano-structured Fibers. Chemical Industry Press: Beijing, 0000.
25. Laperre, J.; Gambichler, T. Photodermatol Photoimmunol Photomed 2003, 19, 11.